

Global Conformational Changes upon Receptor Stimulation in Photoactive Yellow Protein[†]

Wouter D. Hoff,[‡] Aihua Xie,[§] Ivo H. M. Van Stokkum,^{||} Xue-jun Tang,[#] Jechiam Gural,[⊥] Arthur R. Kroon,[⊥] and Klaas J. Hellingwerf^{*⊥}

Department of Biochemistry and Molecular Biology, The University of Chicago, Chicago, Illinois 60637, Department of Physics, Oklahoma State University, Stillwater, Oklahoma 74078, Faculty of Physics and Astronomy, Vrije Universiteit, 1081 HV Amsterdam, The Netherlands, Wyeth-Ayerst Research, 401 North Middletown Road, Pearl River, New York 10965, and Department of Microbiology, E. C. Slater Institute, University of Amsterdam, 1018 WS Amsterdam, The Netherlands

Received March 3, 1998; Revised Manuscript Received July 24, 1998

ABSTRACT: Biological signal transduction starts with the activation of a receptor protein. Two central questions in signaling are the mechanism of activation by a stimulus and the nature and extent of the protein conformational changes involved. We report extensive evidence for the occurrence of large structural changes upon the light activation of photoactive yellow protein (PYP), a eubacterial photosensor. Absorption of a blue photon by the *p*-coumaric acid (pCA) chromophore in pG, the initial state of PYP, results in the formation of pB, a putative signaling state. In the presence of an adequate hydration shell, large structural changes in the protein backbone, involving both solvent accessible and core regions, were detected using Fourier transform infrared (FTIR) difference spectroscopy. A significant part (23%) of the amide groups which are buried in pG become exposed to the solvent in pB, as measured through light-induced H/D exchange, using both electrospray ionization mass spectrometry and FTIR spectroscopy. Exposure of previously buried hydrophobic sites would lead to an increase in heat capacity during pB formation and a decrease in heat capacity during pB decay. Thermodynamic studies indeed show that the heat capacity change of pB activation is -2.35 ± 0.08 kJ/(mol/K), independent of pH from pH 2.4–7.5. A model for photoactivation of PYP is proposed, which provides a framework for a deeper understanding of receptor activation in general.

Biological signal transduction is of paramount importance for the functioning of living organisms. The first component in signal transduction chains is a receptor protein. Stimuli from either within the cell or from its surroundings can convert the receptor into its active conformation: the signaling state. The change in receptor protein conformation that occurs during signaling state formation is thought to be responsible for relay of the signal to the next component in the signal transduction chain, involving protein–protein interactions. To obtain a full understanding of the molecular mechanism of signal transduction, it is essential to study the extent and nature of the structural changes that occur during the formation of the signaling state.

In most cases formation of the signaling state is caused by the binding of a ligand. Activation of photoreceptors is triggered by the absorption of a photon. The light-activated nature of photoreceptors and the often-observed reversibility of the changes elicited are strong experimental advantages,

allowing time-resolved studies and the application of various forms of spectroscopy. Therefore, the most extensive information on receptor activation has been obtained on two photosensory proteins: mammalian rod rhodopsin (1) and sensory rhodopsin I from the Archaeon *Halobacterium salinarum* (2). However, detailed structural studies on the conformational changes that occur during receptor activation have not been reported and are hampered by the lack of high-resolution structural data on these proteins. We employ photoactive yellow protein (PYP)¹ as a powerful model system for studies on the molecular mechanism of receptor activation.

PYP (3, 4) is a novel type of photoreceptor that is small (125 amino acids) and water soluble. It displays an absorbance maximum at 446 nm due to its unique *p*-coumaric acid (pCA) chromophore (5–9). PYP has been indicated to mediate a negative phototaxis response in the phototrophic Eubacterium *Ectothiorhodospira halophila* (10). The PYP from *E. halophila* is the best-studied member of a well-conserved family of proteins, the Xanthopsins (11). The crystal structure of PYP has been determined at 1.4 Å resolution (12), revealing structurally important residues in the chromophore binding pocket.

[†] WDH is supported by the Cancer Research Fund of the Damon Runyon-Walter Winchell Foundation Fellowship DRG-1346. This work was supported by ONR Grant N00014-95-1-0310 to A.X., by a BRSG grant from the Albert Einstein College of Medicine, and by NIH Grant RR09113 to X.T.

^{*} Corresponding author. E-mail: K.Hellingwerf@chem.uva.nl.

[‡] The University of Chicago.

[§] Oklahoma State University.

^{||} Vrije Universiteit.

[#] Wyeth-Ayerst Research.

[⊥] University of Amsterdam.

¹ Abbreviations: PYP, photoactive yellow protein; pCA, *p*-coumaric acid; FTIR, Fourier transform infrared; ESMS, electrospray ionization mass spectrometry.

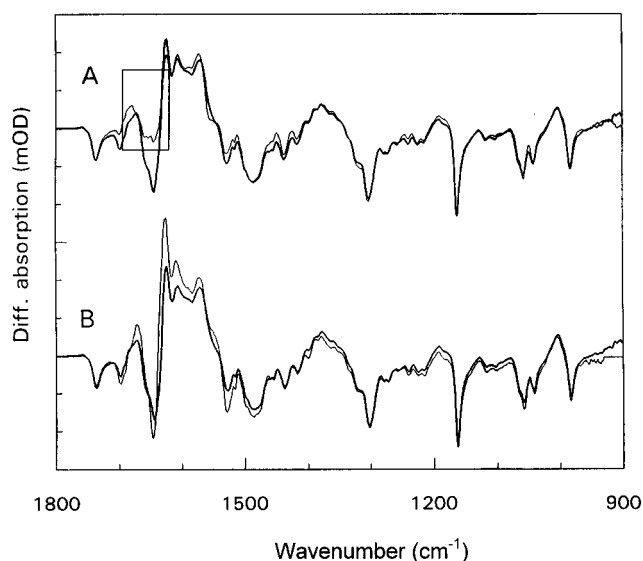


FIGURE 1: FTIR difference spectroscopy of pB formation. Comparisons are shown between the pB – pG difference spectrum recorded for (A) PYP at pH 3.5 in solution using a 15 μ m spacer (thin line) and in a hydrated film (thick line) and for (B) hydrated PYP films at pH 3.5 (thick line) and 7.0 (thin line). For the sample in solution the region distorted by intense H₂O absorbance is indicated by the box. Negative bands indicate vibrational modes from pG, while positive bands correspond to modes in pB. The full scale of the vertical axis is 60 mOD.

PYP displays a rhodopsin-like photocycle involving a primary, red-shifted intermediate pR ($\lambda_{\text{max}} = 465$ nm) that is converted into a long-lived, blue-shifted state pB ($\lambda_{\text{max}} = 355$ nm) on a sub-millisecond time scale (4, 13). On a subsecond time scale, pB returns to the initial state pG. The PYP photocycle is probably initiated by photoisomerization of the pCA chromophore (14, 15), leading to the formation of pR. Subsequently, a proton transfer event occurs in which the pCA accepts a proton from Glu46, leading to the formation of pB (15, 16). During this transition a protein conformational change (17) involving partial unfolding (18) has been proposed to take place. In view of its properties and by analogy with the archaeal sensory rhodopsins, the pB intermediate is likely to be the signaling state of PYP.

Here we present extensive experimental data that qualitatively and quantitatively reveal the nature and extent of the conformational changes that occur upon photoactivation of PYP. Three independent experimental techniques have been employed: (i) Fourier transform infrared (FTIR) difference spectroscopy for probing structural changes in the protein backbone; (ii) light-induced hydrogen–deuterium exchange, monitored by electrospray ionization mass spectrometry (ESMS) and by FTIR spectroscopy, to detect structural changes involving the exposure of buried sites; (iii) thermodynamic studies revealing changes in heat capacity due to the exposure of hydrophobic surface area.

MATERIALS AND METHODS

Sample Preparation. For FTIR spectroscopy and ESMS measurements, a histidine-tagged version of the PYP from *E. halophila* containing the N-terminal extension MRGSH₆-GSD₄K was overproduced in *E. coli* and reconstituted in vitro using the anhydride of pCA (11, 19). PYP obtained in this way displays UV/vis difference spectra indistinguishable from native PYP (Figure 3A). PYP was homogeneously

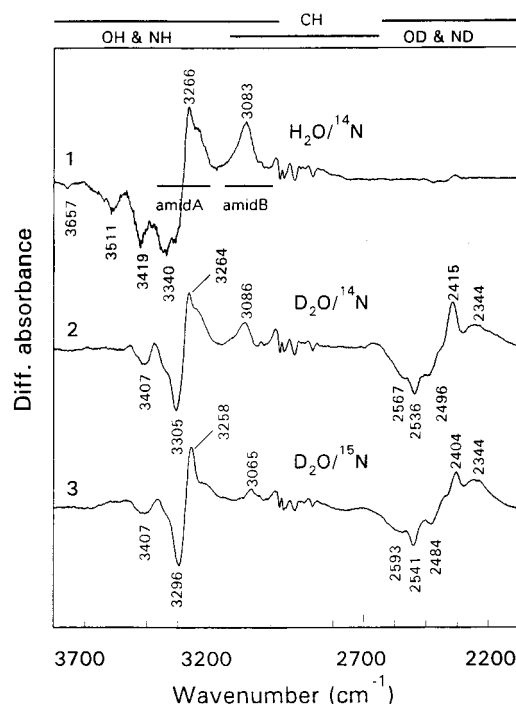


FIGURE 2: The pB – pG FTIR difference absorbance spectrum in the amide A region. The pB – pG difference spectrum in the XH stretching region was recorded for hydrated (trace 1), deuterated (trace 2), and ¹⁵N-labeled deuterated (trace 3) PYP films. The expected regions of absorbance by OH, NH, CH, OD, and ND stretching modes and those of amide A and amide B modes are indicated by bars. The full scale of the vertical axis is 44 mOD. The difference spectra were scaled using sharp negative bands of large amplitude (see Figure 1) arising from the pCA chromophore (our unpublished results).

labeled with ¹⁵N by growing the PYP-overproducing *E. coli* strain in minimal medium with ¹⁵NH₄Cl as the sole nitrogen source. ESMS and NMR spectroscopy indicate >95% of labeling with ¹⁵N in the sample used here (not shown). For experiments on apoPYP the overexpression product was purified without reconstitution (19). PYP used for the thermodynamics measurements was purified from *E. halophila* as described in (ref 3) with the modifications reported in ref 13. For FTIR spectroscopy, PYP samples were centrifuged repeatedly using Microcon filters, to obtain a protein concentration of approximately 4 mM in either 20 mM citric acid at pH 3.5 or in 10 mM potassium phosphate buffer at pH 7.0.

FTIR Spectroscopy. The IR spectra of PYP samples were measured at 2 cm^{-1} resolution in the region of 3800–800 cm^{-1} using a Mattson FTIR spectrometer (Galaxy 5000) with a KBr beam splitter and a liquid nitrogen cooled MCT detector. Hydrated films of PYP were prepared by spreading the PYP solution on a calcium fluoride sample plate as described in ref 15. These films were used for FTIR difference spectroscopy. The pB – pG difference spectra were determined by measuring the effect of steady state illumination of the PYP sample with blue light as described in ref 15. To detect light-induced H/D exchange, a PYP film at pH 3.5 was extensively deuterated in the light at room temperature. The film was then exposed to H₂O in the dark for 45 h at 4 $^{\circ}\text{C}$, allowing D to H exchange of groups exposed in pG. The effect of subsequent illumination on D to H exchange was monitored by calculating difference

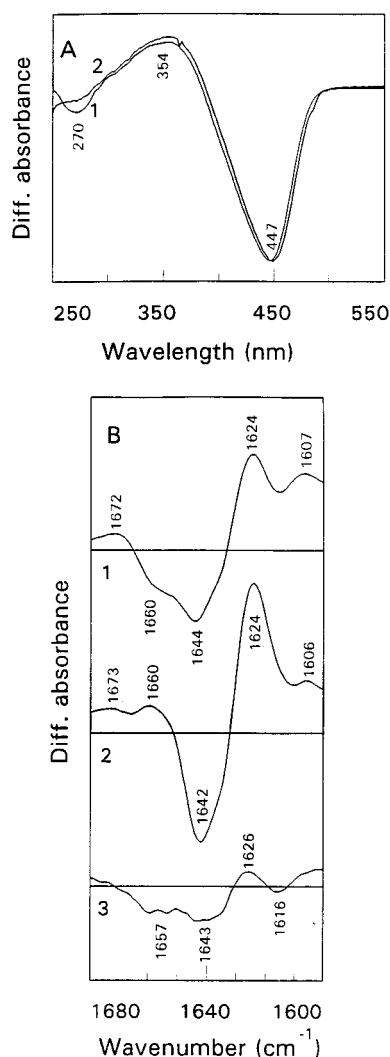


FIGURE 3: The pB – pG difference absorbance spectrum at high and low levels of hydration in the UV/vis and amide I spectral regions: (A) UV/vis difference absorbance spectra associated with the formation of pB at high (trace 1) and low (trace 2) levels of hydration; (B) amide I region of the pB – pG difference spectra for hydrated (trace 1) and deuterated (trace 2) PYP films compared with that obtained for a PYP film at reduced hydration (trace 3). The full scales of the vertical axes are 740 and 95 mOD for panels A and B, respectively.

spectra between two consecutive scans collected in the dark, separated by 2 min of illumination.

Electrospray Ionization Mass Spectrometry. The ES mass spectra of apoPYP and PYP were measured in H₂O, buffered at pH 7 with 20 mM ammonium acetate, and recorded as described in refs 20 and 21. Kinetics of H/D exchange (see refs 20 and 21) in PYP, and apoPYP were determined with and without continuous illumination. This was accomplished by manually diluting the protein solutions 20-fold in D₂O at room temperature, followed by continuous injection of the sample into the mass spectrometer. The dead time of this procedure was approximately 1 min. The data obtained using this method are highly accurate and reproducible after 10 min of mixing, to initiate H/D exchange. Data obtained during the first 10 min are not reported because of the experimental error introduced by uneven mixing. The use of a glass syringe for injection allowed the sample to be illuminated during H to D exchange. The extent of H/D exchange was monitored through the resulting increase in

molecular weight, computed from the changes in m/z of the 7+ and 8+ charged states. For the 8+ charged state of PYP there are 259 exchangeable protons (141 from the backbone and 118 from side chains). With the solvent containing 95% D₂O and 5% H₂O, the maximum number of H/D exchanges per PYP molecule then equals 246.

Thermodynamic Analysis. The kinetics of the pB to pG photocycle transition at reduced pH values was recorded using the kinetic mode of an Aminco 2000 (SLM Instruments) spectrophotometer immediately after a 10 s illumination period. Data analysis and the application of protein folding thermodynamics to the PYP photocycle were performed as described in ref 18.

RESULTS AND DISCUSSION

FTIR Difference Absorption Spectroscopy of pB Formation. FTIR difference absorption spectroscopy is a powerful technique to obtain detailed information on molecular processes occurring during protein function. Here we apply this technique to examine structural changes in the protein backbone of PYP upon photostimulation.

To obtain FTIR difference absorption data with a high signal-to-noise ratio, it is optimal to use well-hydrated protein films at low pH. The use of such films, instead of solution samples, allows detection of signals in important spectral regions (especially the amide A and amide I modes) where water absorbs strongly. The reduced pH value prolongs the lifetime of pB (22), increasing the level of pB accumulation during continuous illumination. Since the preparation of PYP samples at low pH and in hydrated films may introduce unwanted effects on the structural changes during the native functional processes in the PYP photocycle, we performed control experiments to address this issue. Figure 1A shows a comparison of the pB – pG difference spectrum at pH 3.5, in solution and in a hydrated film, in the spectral region from 1800 to 900 cm⁻¹. Outside the regions of water absorption, these two difference spectra strongly resemble each other. In Figure 1B a comparison of the pB – pG difference spectrum in PYP films at pH 3.5 and 7.0 is depicted. Again, the two spectra strongly resemble each other. In view of the high information content of the FTIR difference spectra, it can be concluded that FTIR spectroscopy on well-hydrated PYP films at pH 3.5 accurately reflects molecular events during pB formation in solution at physiological pH.

The pB – pG difference spectra in Figure 1 contain a large number of signals. The large peaks at 1305, 1163, 1058/1041, and 983 cm⁻¹ presumably arise from vibrational modes of the pCA chromophore (7) and will be analyzed elsewhere. Here, we focus on the spectral regions reporting on structural changes in the protein backbone, using the peaks arising from pCA for the scaling of the pB – pG FTIR difference spectra.

Structural Changes in Protein Backbone upon Formation of the pB Intermediate. The frequency, amplitude, and bandwidth of IR absorption bands of the protein backbone are sensitive to hydrogen bonding, polarity of the surroundings, and structural distortion (23, 24). Therefore, FTIR difference spectroscopy is a highly sensitive technique to detect structural changes in protein backbone. In this paper, we examine signals arising from the N–H stretching mode (the amide A region: 3500–3000 cm⁻¹) and from the C=O

stretching mode coupled to the C–N stretching mode (the amide I region: 1690–1620 cm^{-1}).

The pB – pG difference absorption spectrum in the spectral region 3700–2200 cm^{-1} is shown in Figure 2. This spectrum reveals a number of signals in the region from 3700 to 2800 cm^{-1} , where the N–H and O–H (3700–3000 cm^{-1}) and C–H (3100–2700 cm^{-1}) stretching vibrational modes absorb. Major peaks are found at 3511, 3419, 3340, 3266, and 3083 cm^{-1} (Figure 2, trace 1). These signals in the pB – pG difference spectrum are larger than those observed for rod rhodopsin (25) and much larger than those for bacteriorhodopsin (26, 27). This result indicates that large structural changes occur during the formation of pB. Due to possible partial cancellation of positive and negative bands, these signals represent the minimal conformational change occurring during the formation of pB.

To distinguish between contributions from N–H stretching modes and those from O–H and C–H stretching modes, we examined the effects of H/D exchange and ^{15}N -labeling on the signals observed in the pB – pG difference spectrum. Extensive deuteration (in combination with illumination) of the sample leaves the C–H stretching modes unaffected, while a considerable fraction of the O–H and N–H signals in the pB – pG difference spectrum is shifted to lower frequencies, expected for O–D and N–D vibrations (Figure 2, trace 2), with main peaks at 2536, 2415, and 2344 cm^{-1} . However, some OH/NH stretching signals (mainly at 3407, 3305, 3264, and 3086 cm^{-1}) resist H/D exchange. Apparently, the NH and OH groups giving rise to these signals are protected against exchange (28–30). This shows that protein conformational changes in the pG to pB transition occur not only in solvent accessible regions of PYP but also in its core that is protected from H/D exchange.

Contributions from OH and NH groups were distinguished by measuring the effect of homogeneous ^{15}N isotopic labeling of PYP on the pB – pG difference spectrum of a deuterated film (Figure 2, trace 3). The signals at 3305, 3264, and 3086 cm^{-1} shift to 3296, 3258, and 3065 cm^{-1} upon ^{15}N labeling, identifying these bands as amide A and B signals, expected at around 3300 and 3100 cm^{-1} respectively (23). Thus, the majority of the groups resisting H/D exchange are backbone amide groups (28–30). In addition, a number of C–H stretching bands, of lower amplitude, were observed in the range from 3000 to 2800 cm^{-1} . A signal possibly originating from structural water is seen at 3657 cm^{-1} .

Figure 3B depicts the pB – pG difference spectrum in the amide I region. A strong negative peak at 1644 cm^{-1} and a strong positive peak at 1624 cm^{-1} are observed for the PYP film in H_2O (Figure 3B, trace 1). The total integrated intensity of these difference signals (1650–1615 cm^{-1}) is $\sim 2.5\%$ of the total integrated intensity of the amide I peak in this region, a value substantially larger than the one reported for rhodopsin (31) and Ca^{2+} -ATPase (32).

Possible complications in FTIR difference spectroscopy are overlap of different signals and the identification of the modes contributing to the observed signals. In the experiments reported here, we observe signals in the amide A, amide I, and amide II (see below) regions. We probed the signals observed in these regions for their (in)sensitivity to H/D exchange and ^{15}N labeling and can conclude that the signals show the behavior expected for amide modes. In addition, all three regions consistently reveal the occurrence

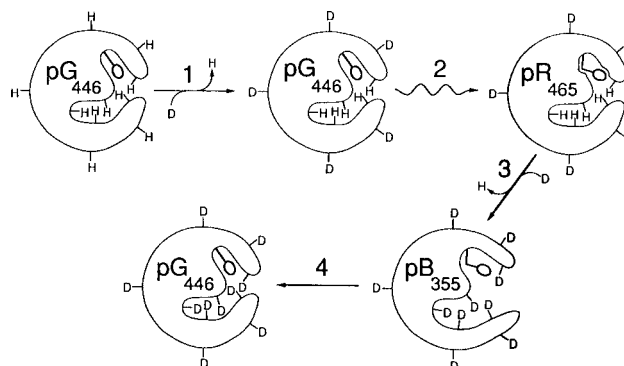


FIGURE 4: Model for light-induced H to D exchange in PYP. The rationale for the detection of conformational changes in PYP upon photoactivation by light-induced H/D exchange is depicted: (1) H to D exchange in pG; (2) subsequent light-induced formation of pR; (3) its conversion to pB, resulting in additional H/D exchange; (4) recovery of pG from pB.

of large changes in backbone conformation during pB formation. Therefore, the spectral indicators for backbone structure in the pB – pG difference spectrum provide direct qualitative evidence for the occurrence of large structural changes during the activation of PYP.

Effect of Reduced Hydration on pB Formation. The effect of a reduction in the level of hydration on the formation of pB was studied. Light-induced difference spectra were obtained for films containing ~ 1000 (high hydration), 600, and 350 (low hydration) molecules of water per PYP molecule (traces 1, 2 and 3, respectively in Figure 3B). Equal contribution by weight of PYP and water to the film would result from 890 water molecules per PYP molecule. Absorbance difference data in the UV/vis region (Figure 3A) indicate the formation of pB (λ_{max} 354 nm) upon illumination under these conditions; at low hydration the negative band at 446 nm is slightly shifted (to 448 nm). At both high and low hydration, difference absorbance data in the IR region (not shown) reveal the presence of various large negative peaks caused by the pCA chromophore.

A reduction in the level of hydration of the PYP film has marked effects on the PYP photocycle: (i) The yield of pB formation is dramatically diminished (to $\sim 20\%$ as compared to the yield at high hydration). (ii) A negative feature at 270 nm in the pB–pG UV/vis difference absorption spectrum, which has been tentatively assigned to changes in the environment of aromatic amino acids (22), is absent (Figure 3A). (iii) The amide I signals are strongly reduced (Figure 3B, trace 3). The strong reduction in the amide I difference signals shows that at low hydration a pB state is formed without the occurrence of large structural changes in protein backbone. This reduction in structural changes is confirmed by the lack of changes in aromatic amino acids as observed through the disappearance of the difference signal at 270 nm.

Exposure of Buried Groups upon pB Formation Revealed by Light-Induced H/D Exchange. The conformational changes that occur upon the formation of pB may lead to the exposure of previously buried sites to the solvent. To probe the existence of sites that are buried in pG and that become exposed to the solvent in pB, we developed a novel method (Figure 4) that is based on the notion that exposed sites readily undergo H/D exchange, while buried sites resist such exchange (28–30). To quantitatively detect this effect we

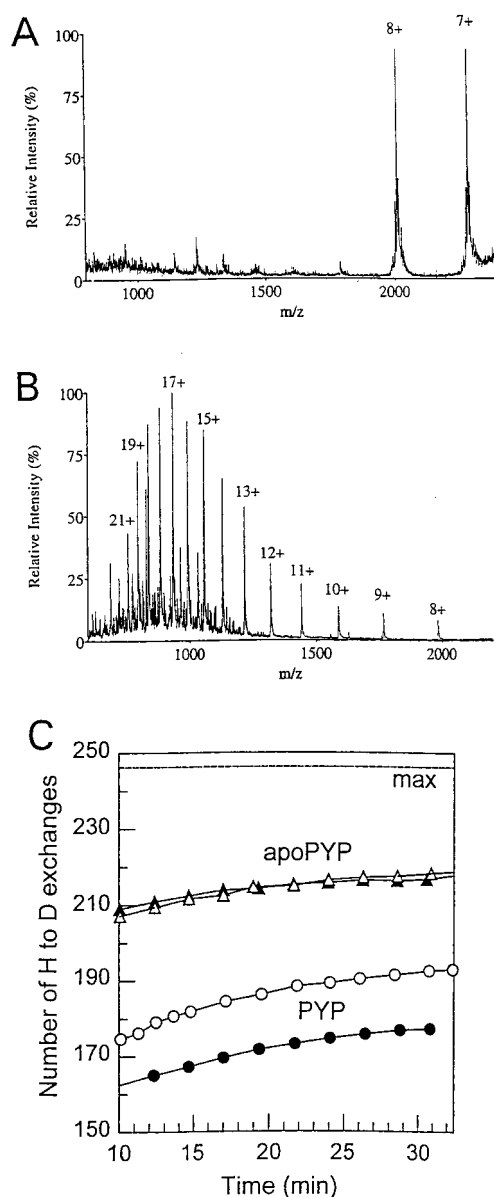


FIGURE 5: H/D exchange in PYP and apoPYP at pH 7 in the dark and during continuous illumination, probed by electrospray ionization mass spectrometry. The ES mass spectra of PYP (A) and apoPYP (B) in H_2O buffered at pH 7 are shown. (C) Kinetics of H to D exchange in PYP (circles) and apoPYP (triangles) in the dark (filled symbols) and during continuous illumination (open symbols) after 20-fold dilution of PYP in D_2O are also shown. The maximum exchange level for PYP is indicated, based on its covalent structure and the dilution factor in D_2O . The level of H to D exchange was calculated from the changes in m/z of the +7 and +8 charge states.

have used ESMS to measure the increase in the mass of PYP at pH 7, as a result of H/D exchange, in the dark and upon photoexcitation.

The ESMS spectrum of a protein reveals both its molecular weight and its net charge. The mass of native PYP at pH 7, measured by ESMS (Figure 5A), corresponds exactly to the mass expected for histidine-tagged PYP. The majority of the PYP molecules were observed to carry 7+ and 8+ charges. Compared to the maximum of 24+ charges based on the amino acid sequence of PYP, the predominant states with 7+ and 8+ charges carry relatively little net charge, which is typical for proteins in their native conformation (see ref 21). In contrast, apoPYP exhibits a wider range of charge states, from 7+ up to 23+ (Figure 5B), with highest

abundance of 17+. This observation indicates that without the pCA chromophore the protein has a more accessible structure.

It is expected that H/D exchange of apoPYP is the same in the dark and upon illumination, since apoPYP has no pCA chromophore and therefore displays no photocycle. Indeed, in our control experiment (Figure 5C, triangles) the exchange curves in the dark and in the light are essentially identical. This result also demonstrates that the light-induced H to D exchange technique we employ is accurate and reproducible.

For native PYP significant differences are observed between H/D exchange in the dark and in the light (Figure 5C, circles). In the dark, 162 out of the 246 exchangeable protons in PYP were deuterated during the first 10 min. This number increased to 177 after 30 min of exchange, while 69 buried sites resisted exchange. In the light, the number of H/D exchanges is 175 of the 246 sites after 10 min and 193 after 30 min. Therefore, in the light the number of buried sites is reduced from 69 to 53.

This result demonstrates that the photoexcitation results in the exchange of 16 additional sites, evidencing and quantifying the existence of light-dependent H/D exchange in PYP. Since no difference in H/D exchange level upon illumination was detected for apoPYP, the observed light-dependent H/D exchange in PYP is caused by photoexcitation of the protein into its photocycle. Comparison of the lifetime of pR ($\sim 250 \mu s$) with the lifetime of pB ($\sim 250 ms$) allows the conclusion that the light-induced H/D exchange effect is caused by the formation of the pB state.

Essentially all of the sites resisting H/D exchange in this experiment (performed at pH 7.0) are expected to be amide protons (28–30). Therefore, a significant fraction of the protected backbone in pG, at least 23% (16/69), becomes more solvent accessible in pB. This is strong quantitative evidence for the occurrence of a major conformational rearrangement during the PYP photocycle.

Since the steady-state concentration of pB is expected to be rather low, at the pH and illumination conditions used in this experiment, the difference in protection against H/D exchange in pG and pB cannot be directly estimated from the data presented in Figure 5B. The kinetics on the order of 10 min at which the 16 light-dependent sites exchange should be regarded as a lower limit for the exchange rate of these sites in pB.

Note that after 30 min the number of exchanged sites in apoPYP is 217, significantly higher than the value of 177 for PYP in the dark. This result confirms the increase in accessibility in apoPYP, as compared to holoPYP. However, apoPYP appears to retain some residual structure, since 30 sites resist H/D exchange.

To obtain independent evidence for the occurrence of light-induced H/D exchange in PYP, we monitored this effect by FTIR difference spectroscopy. A PYP film was (i) first extensively deuterated during illumination, (ii) then dried, and (iii) finally exposed to H_2O vapor in the dark for 45 h resulting in partial D to H exchange. Subsequent measurement of the pB – pG difference spectrum revealed a number of O–D/N–D stretching signals (Figure 6A, trace 1), confirming the presence of conformational changes in sites that resist H/D exchange in pG described above. The negative sign of all of these OD/ND signals in the pB – pG difference spectrum indicates that the sites involved have undergone

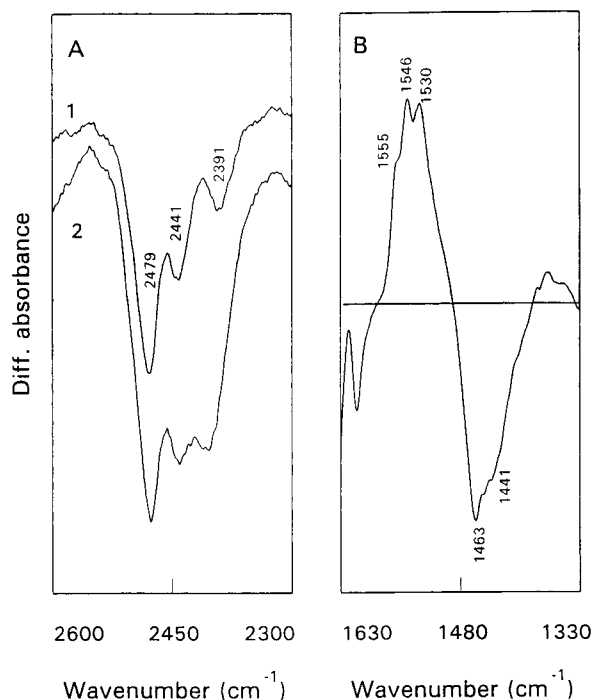


FIGURE 6: Light-induced D to H exchange in PYP probed by FTIR difference absorbance spectroscopy. Difference signals arising from D to H exchange induced by illumination are depicted for two spectral regions: (A) X-D stretching (trace 1 is a pB - pG difference spectrum; trace 2 is the difference between two pG scans separated by 2 min of illumination); (B) the amide II and II' region (calculated as trace 2 in panel A). The full scales of the vertical axes are 4.3 and 15 mOD for panels A and B, respectively.

D to H exchange during the measurement of the difference spectrum. This is confirmed by the difference between two pG spectra of this sample separated by a 2-min period of illumination (Figure 6A, trace 2). Apparently, the sites involved are well protected against H/D exchange in the dark but exchange rapidly upon illumination.

Light-induced D to H exchange signals are also evident in the amide II region (Figure 6B), which is characterized by a $\sim 100\text{ cm}^{-1}$ upshift in frequency upon exchange from deuterium to proton (24). This upshift confirms that the signals arise from amide II vibrational modes. These signals provide independent proof that backbone amide groups, which are buried in pG, rapidly exchange upon the formation of pB.

It should be pointed out that the changes in H/D exchange rate in PYP upon illumination can be caused by a number of effects, including changes in hydrogen bonding, accessibility, and dynamics. Although a more detailed interpretation of this effect in PYP is not possible at this point, the fact that a relatively large fraction of the protected sites in pG are involved strongly indicates the occurrence of major conformational rearrangements during pB formation. The results on light-induced H/D exchange in PYP reported here provide a new and powerful tool to probe protein conformational changes in photoreceptors in general.

Exposure of Hydrophobic Sites in pB Revealed by Thermodynamic Studies. To complement the observation that H/D exchangeable sites which are buried in pG become solvent exposed in pB, we tested the possibility of exposure of hydrophobic sites in pB. This would lead to an increase in heat capacity upon pB formation, resulting in curved Arrhenius plots for the PYP photocycle kinetics (see refs

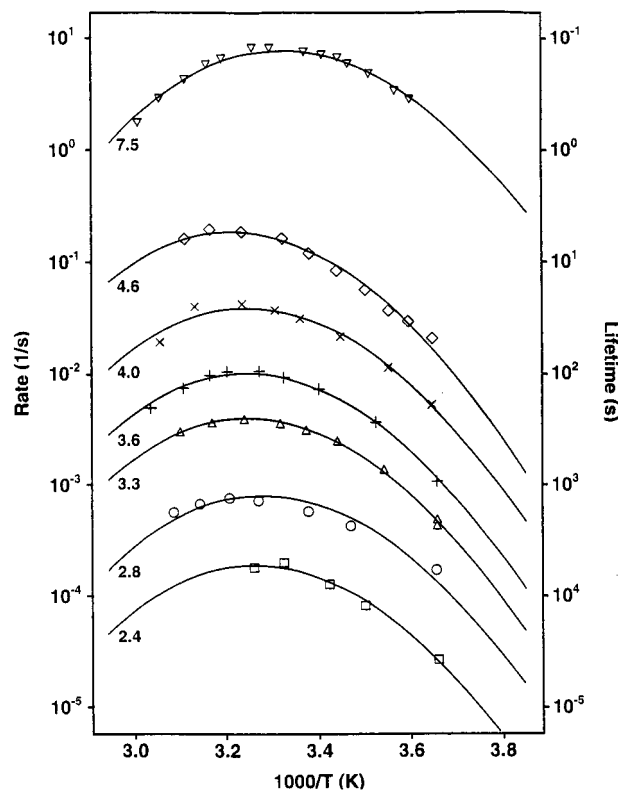


FIGURE 7: Temperature dependence of the pB to pG transition at pH values between 7.5 and 2.4. The temperature dependence of the kinetics of the last PYP photocycle step was determined at the indicated pH values. These data were fitted with a model based on a pH-independent activation change in heat capacity (see text). The fit (resulting in a ΔC_p^\ddagger of $-2.35 \pm 0.08\text{ kJ/(mol/K)}$) is shown by the solid lines. The photocycle kinetics data at pH 7.5 were redrawn from (ref 18).

33 and 34). Indeed, the temperature dependence of the photocycle kinetics strongly deviate from Arrhenius behavior (17), which has been explained in terms of an increase in heat capacity during the formation of pB, using protein folding thermodynamics (18).

In addition to changes in heat capacity, curved Arrhenius plots may be caused by other phenomena, including temperature-dependent equilibria between intermediates. Therefore, it is necessary to distinguish between various alternative explanations. To subject the proposal for the occurrence of heat capacity changes (ΔC_p) during the PYP photocycle to a stringent test, we perturbed the kinetics of the pB to pG transition by varying the pH (see ref 22). On the basis of extensive studies on the unfolding of proteins (33, 34), the model involving heat capacity changes predicts a pH-independent ΔC_p . However, for explanations other than changes in heat capacity, it would be expected that perturbations of the system by external parameters such as pH, etc., would result in a change in the observed "apparent change in heat capacity".

We determined the temperature dependence of the kinetics of the pB to pG photocycle transition (Figure 7) at various pH values between 2.4 and 7.5. These data were analyzed using the following equations, in which ΔC_p^\ddagger is the change

$$\ln K^\ddagger = \frac{\Delta S^\ddagger(T_0)}{R} - \frac{\Delta H^\ddagger(T_0)}{RT} - \frac{\Delta C_p^\ddagger}{R} \left(1 - \frac{T_0}{T} + \ln \frac{T_0}{T} \right)$$

$$K^\ddagger = \frac{kh}{k_b T}$$

in heat capacity for pB activation, T_0 is a reference temperature, h is the Planck constant, k_b is the Boltzmann constant, and k is the experimentally determined rate constant. This analysis revealed that the data obtained over the entire pH range from 2.4 to 7.5 are accurately described by a single heat capacity change of pB activation of -2.35 ± 0.08 kJ/mol/K. Since we affect the rate of the pB to pG transition by 5 orders of magnitude by changing the pH of the solution, the pH-independence of the ΔC_p^\ddagger over this pH range strongly argues against other interpretations of the temperature dependence of the PYP photocycle kinetics.

Other results provide additional support for the occurrence of heat capacity changes during the PYP photocycle. (i) The numerical value obtained for the ΔC_p^\ddagger of the pB to pG transition is of the expected order, as compared to the results of protein denaturation studies. (ii) The effect of organic solvents on the kinetics of the PYP photocycle indicates the exposure of hydrophobic sites in pB (17). (iii) Evidence has been reported which indicates a similarity between pB and the pB_{dark} state which is populated in the dark at low pH values (22). This acid-denatured state of PYP is formed with a heat capacity change of -2.11 ± 0.08 kJ/mol/K (18, 35), i.e., a size similar to the heat capacity changes occurring during the PYP photocycle.

On the basis of these considerations, we conclude that major structural rearrangements occur during pB formation, which involve the exposure of hydrophobic sites, resulting in an increase in heat capacity. This conclusion is supported by two independent lines of evidence reported here: changes in backbone structure upon pB formation observed by FTIR spectroscopy and light-induced changes in H/D exchange. In addition, the frequency downshift in the amide A region and the increase in amide B absorption in the pB – pG difference spectrum (Figure 2) are consistent with the exposure of previously buried backbone amide groups, since these spectral features can be explained by increased hydrogen bonding and increased polarity.

Heat capacity changes are the hallmark of protein folding events (33, 34). While ΔC_p values have been reported for the folding of many proteins, only a few values of the ΔC_p^\ddagger characterizing the transition state of the folding process have been determined (using the temperature dependence of the kinetics of protein folding (36–41)). The ΔC_p^\ddagger value that characterizes the pB to pG transition is in the same order of magnitude as these latter values, indicating that this transition is thermodynamically equivalent to a protein refolding event. This agreement is remarkable, since we have not studied protein denaturation but the light-driven cycle of a photo-sensory protein. The ΔC_p^\ddagger of pB formation is roughly one-third of that expected for the complete unfolding of PYP, indicating the involvement of approximately 40 residues in the conformational change during PYP activation and the exposure of approximately 6200 Å² of hydrophobic surface in pB (33). This corresponds to ~30% of the total surface area of PYP in fully extended conformation, taking the amino acid composition of PYP (9) into consideration.

Model for the PYP Photocycle. The data reported here conclusively demonstrate the occurrence of a global conformational transition in PYP during the formation of pB.

These conformational changes are likely to be involved in signal relay during PYP function in the cell. The mechanism involved in the light-triggered global conformational changes in PYP can be described as follows. From studies on the effect of pH on protein stability a view has emerged in which a change in protonation state in a very small number of structurally important sites at extremes of pH is the cause of (partial) protein unfolding at these pH values (42, 43). These sites are buried within the protein and are characterized by an anomalously shifted pK_a value. In pG the pCA chromophore is buried within the protein (12) and is present as an anion (6–8). In solution, pCA and thiol ester linked pCA model compounds exhibit a pK_a of approximately 8.8 (6, 8, 19), while in pG the apparent pK_a of pCA is shifted to the much lower value of 2.8 in pG (assuming Henderson–Hasselbalch behavior; 3, 22). Therefore, the pCA anion has properties which identify it as a structurally important site. The large shift in pK_a value of the chromophore indicates that interactions between the pCA anion and its binding pocket significantly stabilize the pG state. This leads to the following structural and thermodynamic model for the PYP photocycle: Recent studies (15, 44, 45) indicate that photoactivation of PYP is initiated by photoisomerization of the pCA from a 7-trans 9-s-cis conformation to a 7-cis 9-s-trans conformation, leading to the formation of pR. This mechanism of photoisomerization does not involve a flip of the phenolic ring of pCA but the disruption of the hydrogen bond between the carbonyl C=O of pCA and the backbone NH of Cys69. In the 7-cis 9-s-trans state the hydrogen bond between Glu46 and the phenolic oxygen of the pCA anion is maintained and even becomes stronger (15), leading to the next step: the actual transfer of the proton from the carboxylic group of Glu46 to the phenolic oxygen of pCA (15, 16) after changes in the proton affinity of these two sites (but see ref 45). This intramolecular proton transfer event has dramatic consequences by eliminating the highly favorable interactions between the pCA anion and its binding pocket and by creating two nonstabilized, buried charges in PYP (Glu46 and Arg52).

The strong destabilization of the protein structure, resulting from the proton transfer event described above, triggers the structural rearrangements during pB formation. These structural changes can be observed through: (i) changes in the conformation of the protein backbone, evidenced by exceptionally large amide signals in the pB–pG FTIR difference spectrum; (ii) the exposure of previously buried OH/NH groups, leading to light-induced H/D exchange; (iii) the exposure of previously buried hydrophobic sites, leading to an increase in heat capacity.

Large structural rearrangements in proteins may be inhibited by nonphysiological experimental conditions, such as reduced hydration and reduced temperature. We found that at low levels of hydration a pB state is formed upon photoexcitation, as evidenced from UV/vis absorption data (Figure 3A), which is not accompanied by large structural changes (Figure 3B). Also at low temperatures, large structural changes upon pB formation are suppressed, since the pB – pG difference spectrum recorded at -40 °C (16) reveals amide I signals that are much smaller than those reported here. The feasibility of a dramatic change in the coupling between events in the photoactive site and conformational changes upon a moderate reduction in temperature

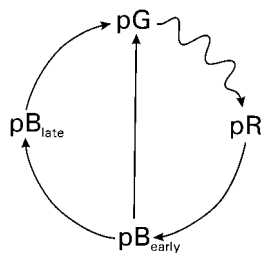


FIGURE 8: Speculative model of the PYP photocycle involving two consecutive pB states. In this proposal a large conformational change occurs during the transition from pB_{early} to pB_{late}.

has been demonstrated (46) for the proton pump bacteriorhodopsin (involving a change in temperature from -13 to -33 °C). For PYP this issue remains to be studied in more detail.

A recent time-resolved X-ray crystallographic study did not reveal a global conformational change during pB formation and indicated that the structural changes are essentially confined to the chromophore binding site of PYP (47). It may be proposed that protein–protein interactions in the crystal lattice are involved in limiting conformational changes during the PYP photocycle. However, since the time-resolved crystallographic experiments on PYP were performed at -12 °C, this reduction in temperature may also contribute. Note that the occurrence of a major conformational transition in the PYP crystals would have prohibited their study by crystallography, since these conformational changes would be expected to result in severe perturbation of crystal order (see ref 48).

On the basis of these considerations, we propose that the formation of the blue-shifted state pB can—depending on the experimental conditions—be associated with either local conformational changes largely limited to the photoactive site of PYP or associated with a large and global conformational change. In the X-ray crystallographic studies (47) and at reduced hydration (Figure 3) small conformational changes occur, while in solution or in well-hydrated films large conformational changes take place during pB formation. A tentative photocycle model incorporating two consecutive pB states is depicted in Figure 8. In this model the formation of an initial pB state (pB_{early}) from pR is accompanied by small conformational changes. Subsequently, this state is converted into a second pB state (pB_{late}) with concomitant large conformational changes. In this model the transition from pB_{early} to pB_{late} can be blocked under some experimental conditions. It remains to be established, however, if the room-temperature photocycle in solution indeed involves two consecutive pB states and if in that case the pB state observed in the X-ray crystallographic experiments corresponds to the early pB state.

The determination of detailed photocycle schemes of PYP under various conditions is beyond the scope of this study. Here, we characterize the nature and extent of the conformational changes that occur during the formation of the pB photocycle intermediate that is formed at physiological temperatures and in solution (or in well hydrated films). Strong evidence is provided for large structural changes during the pG to pB transition. These conformational rearrangements may be the molecular basis for signal generation in PYP.

ACKNOWLEDGMENT

We thank Prof. R. Kaptein for donation of the $^{15}\text{NH}_4\text{Cl}$. W.D.H. thanks Prof. J. L. Spudich for his support.

REFERENCES

1. Rao, R., and Orian, D. D. (1996) *Annu. Rev. Biophys. Biomol. Struct.* 25, 287–314.
2. Hoff, W. D., Jung, K.-H., and Spudich, J. L. (1997) *Annu. Rev. Biophys. Biomol. Struct.* 26, 221–258.
3. Meyer, T. E. (1985) *Biochim. Biophys. Acta* 806, 175–183.
4. Meyer, T. E., Yakali, E., Cusanovich, M. A., and Tollin, G. (1987) *Biochemistry* 26, 418–423.
5. Hoff, W. D., Düx, P., Hård, K., Devreese, B., Nugteren-Roodzant, I. M., Crielard, W., Boelens, R., Kaptein, R., Van Beeumen, J., and Hellingwerf, K. J. (1994) *Biochemistry* 33, 13959–13962.
6. Baca, M., Borgstahl, G. E. O., Boissinot, M., Burke, P. M., Williams, W. R., Slater, K. A., and Getzoff, E. D. (1994) *Biochemistry* 33, 14369–14377.
7. Kim, M., Mathies, R. A., Hoff, W. D., and Hellingwerf, K. J. (1995) *Biochemistry* 34, 12669–12672.
8. Hoff, W. D., Devreese, B., Fokkens, R., Nugteren-Roodzant, I. M., Van Beeumen, J., Nibbering, N., and Hellingwerf, K. J. (1996) *Biochemistry* 35, 1274–1281.
9. Van Beeumen, J., Devreese, B., Van Bun, S., Hoff, W. D., Hellingwerf, K. J., Meyer, T. E., McRee, D. E., and Cusanovich, M. A. (1993) *Protein Sci.* 2, 1114–1125.
10. Sprenger, W. W., Hoff, W. D., Armitage, J. P., and Hellingwerf, K. J. (1993) *J. Bacteriol.* 175, 3096–3104.
11. Kort, R., Hoff, W. D., Van West, M., Kroon, A. R., Hoffer, S. M., Vlieg, K. H., Crielard, W., Van Beeumen, J. J., and Hellingwerf, K. J. (1996) *EMBO J.* 15, 3209–3218.
12. Borgstahl, G. E. O., Williams, D. R., and Getzoff, E. D. (1995) *Biochemistry* 34, 6278–6287.
13. Hoff, W. D., Van Stokkum, I. H. M., Van Ramesdonk, H. J., Van Brederode, M. E., Brouwer, A. M., Fitch, J. C., Meyer, T. E., Van Grondelle, R., and Hellingwerf, K. J. (1994) *Biophys. J.* 67, 1691–1705.
14. Kort, R., Vonk, H., Xu, X., Hoff, W. D., Crielard, W., and Hellingwerf, K. J. (1996) *FEBS Lett.* 382, 73–78.
15. Xie, A., Hoff, W. D., Kroon, A. R., and Hellingwerf, K. J. (1996) *Biochemistry* 35, 14671–14678.
16. Imamoto, Y., Mihara, K., Hisatomo, O., Kataoka, M., Tokunaga, F., Bojkova, N., and Yoshihara, K. (1997) *J. Biol. Chem.* 272, 12905–12908.
17. Meyer, T. E., Tollin, G., Hazzard, J. H., and Cusanovich, M. A. (1989) *Biophys. J.* 56, 559–564.
18. Van Brederode, M. E., Hoff, W. D., Van Stokkum, I. H. M., Groot, M.-L., and Hellingwerf, K. J. (1996) *Biophys. J.* 71, 365–380.
19. Kroon, A. R., Hoff, W. D., Fennema, H., Gijzen, J., Koomen, G.-J., Verhoeven, J. W., Crielard, W., and Hellingwerf, K. J. (1996) *J. Biol. Chem.* 271, 31949–31956.
20. Wang, F., Blanchard, S. J., and Tang, X.-J. (1997) *Biochemistry* 36, 3755–3759.
21. Wang, F., Tang, X.-J. (1996) *Biochemistry* 35, 4069–4078.
22. Hoff, W. D., Van Stokkum, I. H. M., Gural, J., and Hellingwerf, K. J. (1997) *Biochim. Biophys. Acta* 1322, 151–162.
23. Arrondo, J. L. R., Muga, A., Castresana, J., and Goñi, M. (1993) *Prog. Biophys. Mol. Biol.* 59, 23–56.
24. Jackson, M., and Mantsch, H. H. (1995) *Crit. Rev. Biochem. Mol. Biol.* 30, 95–120.
25. Maeda, A., Ohkita, Y. J., Sasaki, J., Shichida, Y., and Yoshizawa, T. (1993) *Biochemistry* 32, 12033–12038.
26. Chang, C.-W., Sekiya, N., and Yoshihara, K. (1991) *FEBS Lett* 287, 157–159.
27. Maeda, A., Sasaki, J., Shichida, Y., and Yoshizawa, T. (1992) *Biochemistry* 31, 462–467.
28. Englander, S. W., Sosnick, T. R., Englander, J. J., and Mayne, L. (1996) *Curr. Opin. Struct. Biol.* 6, 18–23.
29. Woodward, C. (1993) *TIBS* 18, 359–360.

30. Creighton, T. E. (1993) *Proteins, structures and molecular properties*, 2nd ed., pp 282–286, Freeman, New York.
31. Rothschild, K. J., Cantore, W. A., and Marrero, H. (1983) *Science* 219, 1333–1335.
32. Barth, A., Von Germar, F., Kreutz, W., and Mäntele, W. (1996) *J. Biol. Chem.* 271, 30637–30646.
33. Privalov, P. L. (1992) in *Protein folding* (Creighton, T. E., Ed.) pp 83–126, W. H. Freeman, New York.
34. Privalov, P. L., and Gill, S. J. (1988) *Adv. Prot. Chem.* 39, 191–234.
35. Van Stokkum, I. H. M., Gural, J., Hoff, W. D., Van Brederode, M. E., and Hellingwerf, K. J. (1996) *Prog. Biophys. Mol. Biol.* 65 (suppl. 1), 59.
36. Segawa, S., and Sugihara, M. (1984) *Biopolymers* 23, 2473–2488.
37. Chen, B., Baase, W. A., and Schellman, J. A. (1989) *Biochemistry* 28, 691–699.
38. Jackson, S. E., and Fehrst, A. R. (1991) *Biochemistry* 30, 10436–10443.
39. Alexander, P., Orban, J., and Bryan, P. (1992) *Biochemistry* 31, 7243–7248.
40. Schindler, T., and Schmid, F. X. (1996) *Biochemistry* 35, 16833–16842.
41. Sosnick, T. R., Mayne, L., and Englander, S. W. (1996) *Proteins* 24, 413–426.
42. Honig, B., and Yang, A.-S. (1995) *Adv. Prot. Chem.* 46, 27–58.
43. Yang, A.-S., and Honig, B. (1993) *J. Mol. Biol.* 231, 459–474.
44. Genick, U. K., Soltis, S. M., Kuhn, P., Canestrelli, I. L., Getzoff, E. D. (1998) *Nature* 392, 206–209.
45. Perman, B., Šrajer, V., Ren, Z., Teng, T.-Y., Pradervand, C., Ursby, T., Bourgeois, D., Schotte F., Wulff, M., Kort, R., Hellingwerf, K. J., Moffat, K. (1998) *Science* 279, 1946–1950.
46. Ormos, P. (1991) *Proc. Natl. Acad. Sci. U.S.A.* 88, 473–477.
47. Genick, U. K., Borgstahl, G. E. O., Ng, K., Ren, Z., Pradervand, C., Burke, P. M., Šrajer, V., Teng, T.-Y., Schildkamp, W., McRee, D. E., Moffat, K., and Getzoff, E. D. (1997) *Science* 275, 1471–1475.
48. Moffat, K. (1989) *Annu. Rev. Biophys. Biophys. Chem.* 18, 309–332.

BI980504Y